

Skeletal Effects of Estrogen Are Mediated by Opposing Actions of Classical and Nonclassical Estrogen Receptor Pathways

Farhan A Syed,¹ Ulrike IL Mödder,¹ Daniel G Fraser,¹ Thomas C Spelsberg,² Clifford J Rosen,³ Andree Krust,⁴ Pierre Chambon,⁴ J Larry Jameson,⁵ and Sundeep Khosla¹

ABSTRACT: ER α acts either through classical (ERE-mediated) or nonclassical (non-ERE) pathways. The generation of mice carrying a mutation that eliminates classical ER α signaling presents a unique opportunity to study the relative roles of these pathways in bone. This study defines the skeletal phenotype and responses to ovariectomy and estrogen replacement in these mice.

Introduction: Estrogen receptor α (ER α) can act either through classical estrogen response elements (EREs) or through non-ERE (nonclassical) pathways. To unravel these in bone, we crossed mice heterozygous for a knock-in mutation abolishing ERE binding (nonclassical ER α knock-in [NERKI]) with heterozygote ER α knockout mice and studied the resulting female ER $\alpha^{+/+}$, ER $\alpha^{+/NERKI}$, and ER $\alpha^{-/NERKI}$ mice. The only ER α present in ER $\alpha^{-/NERKI}$ mice is incapable of activating EREs but can signal through nonclassical pathways, whereas ER $\alpha^{+/NERKI}$ mice may have a less drastic alteration in the balance between classical and nonclassical estrogen signaling pathways.

Materials and Methods: BMD was measured using DXA and pQCT at 3 months of age ($n = 46$ – 48 /genotype). The mice were randomly assigned to sham surgery, ovariectomy, ovariectomy + estradiol (0.25 μ g/day), or ovariectomy + estradiol (1.0 μ g/day; $n = 10$ – 12 /group) and restudied 60 days later.

Results and Conclusions: At 3 months of age, both the ER $\alpha^{+/NERKI}$ and ER $\alpha^{-/NERKI}$ mice had deficits in cortical, but not in trabecular, bone. Remarkably, changes in cortical bone after ovariectomy and estrogen replacement in ER $\alpha^{-/NERKI}$ mice were the opposite of those in ER $\alpha^{+/+}$ mice. Relative to sham mice, ovariectomized ER $\alpha^{-/NERKI}$ mice gained more bone (not less, as in ER $\alpha^{+/+}$ mice), and estrogen suppressed this increase (whereas augmenting it in ER $\alpha^{+/+}$ mice). Estrogen also had opposite effects on bone formation and resorption parameters on endocortical surfaces in ER $\alpha^{-/NERKI}$ versus ER $\alpha^{+/+}$ mice. Collectively, these data show that alteration of the balance between classical and nonclassical ER α signaling pathways leads to deficits in cortical bone and also represent the first demonstration, in any tissue, that complete loss of classical ERE signaling can lead to paradoxical responses to estrogen. Our findings strongly support the hypothesis that there exists a balance between classical and nonclassical ER α signaling pathways, which, when altered, can result in a markedly aberrant response to estrogen.

J Bone Miner Res 2005;20:1992–2001. Published online on July 18, 2005; doi: 10.1359/JBMR.050713

Key words: bone, osteoporosis, sex steroids

INTRODUCTION

ESTROGEN (E) is critical for the growth and maintenance of the skeleton in humans and in rodents.⁽¹⁾ The effects of E in various tissues, including bone, are mediated by two related receptors, estrogen receptor (ER) α and β .⁽²⁾ Whereas ER α seems to be the major ER mediating E effects on bone,⁽³⁾ ER β also plays a significant role, particu-

larly in trabecular bone.^(3,4) Indeed, studies in human and in rodent bone have found that, whereas cortical bone predominantly contains ER α , trabecular bone contains both ER α and β .^(5–7) Moreover, whereas ER β is generally inhibitory to ER α action⁽⁸⁾; under certain circumstances, it can either substitute for⁽⁴⁾ or enhance⁽³⁾ ER α action.

E can modulate gene transcription through either ER α or β using a number of signaling pathways. The “classical” pathway involves direct DNA binding of the liganded ER to E response elements (EREs),⁽⁹⁾ as in the case of the *prolactin*,⁽¹⁰⁾ *progesterone receptor*,⁽¹¹⁾ and *c-fos*⁽¹²⁾ genes. In addition, however, the ER can also regulate gene expres-

Dr Rosen has received support and served as a principle investigator for Allclix, Aventis, Eli Lilly and Company, GlaxoSmith-Kline, Merck & Co., NPS Pharmaceuticals, and Wyeth. All other authors have no conflicts of interest.

¹Endocrine Research Unit, Mayo Clinic College of Medicine, Rochester, Minnesota, USA; ²Department of Biochemistry and Molecular Biology, Mayo Clinic College of Medicine, Rochester, Minnesota, USA; ³The Jackson Laboratory, Bar Harbor, Maine, USA; ⁴Institut de Génétique et de Biologie Moléculaire et Cellulaire, Institut Clinique de la Souris, CNRS/INSERM/ULP, Collège de France, Illkirch Cedex, France; ⁵Department of Endocrinology, Northwestern University, Chicago, Illinois, USA.

sion through a number of “nonclassical” pathways that do not involve direct DNA binding by the ER but rather are caused by specific protein–protein interactions. Thus, the ER can upregulate the expression of promoters containing activating protein (AP)-1 sites, as in the case of the *collagenase*⁽¹³⁾ and *IGF-I*⁽¹⁴⁾ genes. Similarly, suppression of *IL-6* gene expression by E occurs through interactions of the liganded ER with the NF- κ B complex.⁽¹⁵⁾ Finally, E can also regulate gene expression through membrane actions that involve alterations in MAP kinase activity⁽¹⁶⁾; these effects seem to be particularly important for the antiapoptotic effects of E on osteoblasts.⁽¹⁷⁾ Indeed, it has been suggested that these “nongenotropic” actions of E are largely responsible for E action on bone, with signaling through the classical pathway, while important for reproductive tissues, being largely irrelevant for nonreproductive tissues such as bone.⁽¹⁸⁾

Until recently, it has not been possible to assess the relative contributions of classical signaling requiring direct ER binding to DNA versus nonclassical signaling pathways toward E action in any tissue, including bone. The recent generation of nonclassical ER knock-in (NERKI) mice by Jakacka et al.,⁽¹⁹⁾ however, has provided a unique opportunity to define the significance of these pathways for E action on bone. These mice have a two amino acid substitution (E207A/G208A) in the first zinc finger of the DNA binding domain in one of the ER α alleles. In vitro, this mutant receptor fails to activate reporter constructs containing EREs, but is active in regulating transcription from an AP1 site^(19,20) and retains the ability to interact with Jun in a mammalian cell two-hybrid assay.⁽²⁰⁾ Thus, this mutant receptor lacks the ability to signal through classical EREs, but can signal normally through nonclassical pathways through protein–protein interactions. Whereas heterozygote male mice possessing one wildtype and one NERKI allele are fertile, heterozygote females are infertile and have cystic changes in the ovaries and uterus, along with defects in mammary gland development,⁽¹⁹⁾ suggesting that even in the presence of a wildtype ER α allele, alterations in the balance of classical versus nonclassical ER α signaling have clear biological effects in vivo.

In these studies, we sought to define the relative contributions of classical versus nonclassical ER α signaling toward E action on bone. To do so, we circumvented the problem of infertility in the heterozygote female NERKI mice and generated mice in whom the only ER α mediating E effects on bone and other tissues was the NERKI receptor by crossing heterozygote male ER $\alpha^{+/\text{NERKI}}$ with heterozygote female ER α knock out (ER $\alpha^{-/-}$) mice.⁽²¹⁾ Thus, we analyzed both the basal skeletal phenotype as well as the response to ovariectomy (OVX) and E replacement in the resultant ER $\alpha^{+/+}$ mice (which had both wildtype ER α alleles), ER $\alpha^{+/\text{NERKI}}$ mice (in which there was one wildtype and one NERKI allele), and ER $\alpha^{-/\text{NERKI}}$ mice (in which the only ER α present was the NERKI receptor). In addition, responses to OVX and E replacement in the ER $\alpha^{+/+}$ versus the ER $\alpha^{-/\text{NERKI}}$ mice were placed in the context of complete ER α knockout mice (ER $\alpha^{-/-}$).⁽²¹⁾

MATERIALS AND METHODS

Generation, breeding, and care of animals

Heterozygote NERKI male (ER $\alpha^{+/\text{NERKI}}$) mice⁽¹⁹⁾ in a 129SvJ background were crossed with heterozygote ER $\alpha^{+/-}$ female mice in a C57BL/6 background.⁽²¹⁾ The F1 generation female ER $\alpha^{+/+}$, ER $\alpha^{+/\text{NERKI}}$, and ER $\alpha^{-/\text{NERKI}}$ mice on an identical 50:50 C57BL/6:129SvJ mix were studied. All relevant comparisons were made within these three groups. In addition, the changes in the ER $\alpha^{+/+}$ versus the ER $\alpha^{-/\text{NERKI}}$ mice after various treatments were placed in the context of the corresponding changes in the ER $\alpha^{-/-}$ versus their wildtype ER $\alpha^{+/+}$ control mice. To generate ER $\alpha^{-/-}$ mice, heterozygote male and female ER $\alpha^{+/-}$ mice (both in a C57BL/6 background) were crossed. Note that the ER $\alpha^{-/-}$ mice represent a complete knockout of ER α .⁽²¹⁾ Because the ER $\alpha^{-/-}$ mice were on a different genetic background (C57BL/6) compared with the ER $\alpha^{-/\text{NERKI}}$ mice (F1 50:50 C57BL/6:129SvJ), all statistical comparisons were between the ER $\alpha^{+/\text{NERKI}}$ or ER $\alpha^{-/\text{NERKI}}$ and their corresponding ER $\alpha^{+/+}$ littermates and the ER $\alpha^{-/-}$ and their corresponding ER $\alpha^{+/+}$ littermates. The animals were housed in a temperature controlled room (22 \pm 2°C) with a daily 12-h light/12-h dark schedule. During the experiments, animals had free access to water and were pair fed a soy-free casein based diet (AIN 93M Diets, Bethlehem, PA, USA). Pups were genotyped at 4–5 weeks of age by PCR as described previously.^(19,21) The Institutional Animal Care and Use Committee approved all animal procedures.

Study design

Baseline bone phenotypic characterization: Three-month-old female ER $\alpha^{+/+}$, ER $\alpha^{+/\text{NERKI}}$, and ER $\alpha^{-/\text{NERKI}}$ mice were scanned by DXA at the femur and spine to obtain areal BMDs (aBMDs) and by pQCT at the tibial metaphysis and diaphysis to obtain volumetric BMDs (vBMDs) and other bone-related parameters to define the basal bone phenotype ($n = 46$ –48/genotype). In addition, a subset of the mice ($n = 10$ –12/genotype) also had ex vivo QCT scans of the lumbar spine performed at 5 months of age as well as bone histomorphometric studies of the lumbar spine ($n = 9$ –10/group). Femur lengths were measured using calipers at the time of death at 5 months.

Effect of gonadectomy and E replacement: To compare the skeletal response to OVX and E replacement, the mice were randomly assigned to one of four groups ($n = 10$ –12/group): sham-operated, vehicle pellet implanted (sham); OVX, vehicle pellet implanted (OVX + V); and OVX, estradiol (E₂) pellet implanted (OVX + E). For the E replacement, we used two doses of E₂: one in the clearly physiological range (E_{0.25}, 0.25 μ g/day, 0.015 mg/60 day pellets) and a second, higher dose in the supraphysiological range (E_{1.0}, 1.0 μ g/day, 0.060 mg/60 day pellets). These doses of E were based on an earlier, dose–response study.⁽⁷⁾ Appropriate surgical procedures were carried out, and pellets (Innovative Research of America, Sarasota, FL, USA) were implanted near the right shoulder blade. The mice received calcein injections (10 mg/kg) on days 0 and 56, as well as a tetracycline injection (10 mg/kg) on day 48. BMD was again

measured by DXA and pQCT on day 60. The animals were bled by cardiac puncture and killed by inhalation of CO₂, and tissues were harvested. The uterus was excised and weighed, and the lumbar spine (L₁–L₄), tibiae, and femurs were excised.

BMD measurements

The mice were anesthetized with Avertin (2,2,2 tribromoethanol, 720 mg/kg IP). DXA measurements were carried out using a Lunar PIXImus densitometer (software version 1.44.005; Lunar Corp., Madison, WI, USA). Mice were placed on an animal tray in a prone position, and whole body scans were carried out. After scanning, regions of interest (right femur and lumbar spine [L₁–L₄]) were analyzed. The CVs for the lumbar and femoral BMD were 7.9% and 6.3%, respectively. pQCT measurements were performed with the mice placed in a supine position on a gantry using the Stratec XCT Research SA Plus using software version 5.40 (Norland Medical Systems, Fort Atkinson, WI, USA). Slice images were measured at 1.9 mm (corresponding to the proximal tibial metaphysis) and at 9 mm (corresponding to the diaphysis of the tibia) from the proximal end of the tibia. For trabecular bone, the threshold was set at 480 mg/cm³ and for cortical bone at 710 mg/cm³. The CV was 6.9% for the total tibial vBMD at the metaphysis and 3.9% for the total tibial vBMD at the diaphysis. Ex vivo lumbar spine scans were performed by placing the spines in a plastic tube filled with 70% ethanol with the dorsal surface facing upward. Two vertebral slices were scanned and total, trabecular, and cortical vBMDs were calculated using a modified algorithm.⁽²²⁾

Cortical and trabecular bone histomorphometry

The tibiae and lumbar spines (L₁–L₄) were processed for histomorphometry as previously described.⁽⁷⁾ For calculating the endocortical mineral apposition rates (MARs), 150- μ m-thick cross-sections of the tibial diaphysis, at the tibiofibular junction toward the distal side of the tibia (at approximately the same site where pQCT measurements were taken), were cut using a diamond-edge saw (Isomet; Buehler, Lake Bluff, IL, USA). These unstained sections were ground on a roughened glass surface to a 25 μ m thickness for visualization of the fluorochrome labels under UV light. The MAR was calculated by dividing the interlabel width in micrometers by the time between the labels; in cortical bone in the adult mice, as noted previously,⁽²³⁾ we could not resolve the labels given 6 days apart, and used the labels given at the beginning and end of the study. To assess resorption surfaces, longitudinal cuts of the proximal tibiae were embedded in methyl-methacrylate, sectioned, and stained using Goldner's stain. Erosion on the endosteal surface of the cortical midshaft was calculated by dividing the total eroded perimeter by the total bone perimeter and expressed as a percentage. For trabecular bone measurements, the lumbar spines (L₁–L₄) were stained with Goldner's stain, and the percent bone volume/total volume (%BV/TV) was calculated. All histomorphometric measurements were performed with the OsteoMeasure Analysis System (OsteoMetrics, Atlanta, GA, USA).

μ CT scans

The left femurs were collected 60 days after the surgeries and stored at -80° C. Before the scans, the femurs were slowly thawed in ice-cold 70% ethanol and kept in ethanol during the scan. The femurs were scanned at a resolution of 11 μ m using a μ CT system (Physiological Imaging Research Laboratory, Mayo Clinic, Rochester, MN, USA) in all three dimensions, essentially as described by Jorgensen et al.⁽²⁴⁾

Serum E₂ and IGF-I measurements

Serum E₂ was measured by radioimmunoassay (RIA; Diagnostic Products Corp., Los Angeles, CA, USA). The interassay CV was <10%. Serum IGF-I was measured using an IGF-1 (IGFBP-blocked) RIA kit (American Laboratory Products, Windham, NH, USA). The interassay CV was <6%.

Statistical methods

All data are presented as mean \pm SE. For the baseline measurements, the genotypes were compared with the ER $\alpha^{+/+}$ controls using a two-tailed *t*-test. Additionally, two-tailed *t*-tests were also done to compare the ER $\alpha^{+/NERKI}$ and ER $\alpha^{-/NERKI}$ mice. For the OVX study, the primary analysis was an ANOVA model that evaluated treatment versus genotype interactions for each genotype versus the ER $\alpha^{+/+}$ controls. In secondary analyses, we compared the sham and E-treated groups to the OVX group within a genotype using two-tailed *t*-tests. *p* < 0.05 was considered significant.

RESULTS

Baseline skeletal phenotype

ER $\alpha^{+/NERKI}$ and the ER $\alpha^{-/NERKI}$ mice had similar femur lengths (14.9 \pm 0.1 and 14.7 \pm 0.1 mm, respectively), but both were reduced compared with their wildtype ER $\alpha^{+/+}$ littermates (16.0 \pm 0.2 mm; *p* < 0.001) at 5 months of age. To assess whether mice harboring the NERKI allele also had reductions in bone mass in the axial and/or appendicular skeleton, we measured total BMD at three independent sites: the femur and lumbar spine (L₁–L₄) using DXA (aBMD) and the tibial metaphysis using pQCT (vBMD). As shown in Fig. 1, the ER $\alpha^{+/NERKI}$ and the ER $\alpha^{-/NERKI}$ mice had significantly reduced total BMDs at all three sites compared with their wildtype ER $\alpha^{+/+}$ littermates. Moreover, in the ER $\alpha^{-/NERKI}$ mice, the decrease in BMD at all the sites was even more pronounced compared with the heterozygote ER $\alpha^{+/NERKI}$ mice. The ER $\alpha^{-/-}$ mice did not have reductions in femur or lumbar spine aBMD, but the total vBMD at the tibial metaphysis was significantly reduced relative to their wildtype ER $\alpha^{+/+}$ littermates.

To evaluate whether the osteopenic phenotype was bone compartment specific, vBMD of trabecular and cortical bone was separated by in vivo pQCT measurements at the tibia. Also, because the spine contains both trabecular and cortical compartments (the latter including the cortical rim and posterior elements), we used ex vivo QCT scanning to separate out the trabecular from the cortical spine compo-

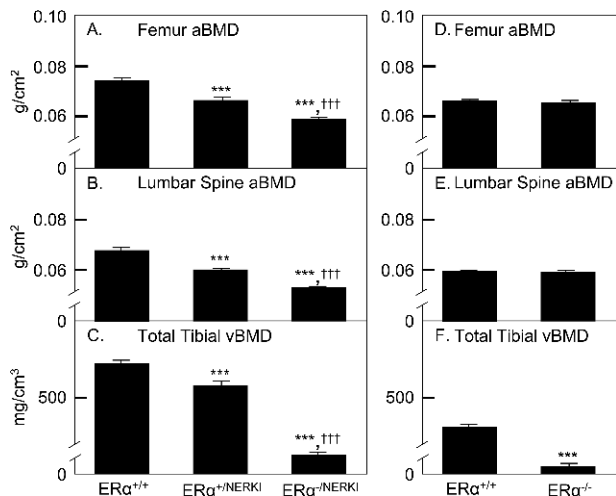


FIG. 1. Baseline total aBMD measurements using DXA scans of (A and D) the femur, (B and E) lumbar spine, and (C and F) total tibial vBMD using pQCT at the metaphysis ($n = 46\text{--}48/\text{genotype}$). $***p < 0.001$ vs. the respective $ER\alpha^{+/+}$ and $†††p < 0.001$ vs. $ER\alpha^{+/NERKI}$ mice.

nents of lumbar vertebrae excised from sham-operated mice at the end of the study. As shown in Fig. 2A, trabecular vBMD at the proximal tibial metaphysis was slightly higher in the $ER\alpha^{+/NERKI}$ compared with the $ER\alpha^{+/+}$ mice, but similar in the $ER\alpha^{-/NERKI}$ and $ER\alpha^{+/+}$ mice. Consistent with the trabecular vBMD data at the tibia, trabecular vBMD at the spine was preserved in the $ER\alpha^{+/NERKI}$ and $ER\alpha^{-/NERKI}$ mice (Fig. 2B). The preservation of trabecular bone in the $ER\alpha^{-/NERKI}$ mice was further confirmed using bone histomorphometry. In this analysis, %BV/TV in the lumbar spine was no different in the $ER\alpha^{-/NERKI}$ ($18.4 \pm 2.0\%$) compared with the $ER\alpha^{+/+}$ mice ($21.2 \pm 4.0\%$, $p = \text{not significant}$). As also shown in Figs. 2C and 2D, trabecular vBMD at the tibial metaphysis and the spine was increased in the $ER\alpha^{-/-}$ mice relative to their $ER\alpha^{+/+}$ littermates.

In contrast to their preserved (or increased) trabecular vBMD, cortical vBMDs at the tibial metaphysis (Fig. 3A) and diaphysis (Fig. 3B) and in the cortical shell and posterior elements of the lumbar spine (Fig. 3C) were significantly reduced in the $ER\alpha^{+/NERKI}$ and $ER\alpha^{-/NERKI}$ mice compared with their $ER\alpha^{+/+}$ controls. In addition, the observed defects in cortical vBMD at the tibial metaphysis and diaphysis and in the cortical elements of the lumbar vertebrae were much more pronounced in the $ER\alpha^{-/NERKI}$ compared with the $ER\alpha^{+/NERKI}$ mice. That the defect was, indeed, localized to cortical bone was further confirmed by measuring other cortical bone parameters (Table 1). At both the tibial metaphysis and diaphysis, the NERKI mice ($ER\alpha^{+/NERKI}$ and $ER\alpha^{-/NERKI}$) exhibited reduced cortical areas and thicknesses in comparison with the control $ER\alpha^{+/+}$ mice. The periosteal bone circumferences at these sites were also significantly reduced in the $ER\alpha^{+/NERKI}$ and the $ER\alpha^{-/NERKI}$ mice. The endocortical circumference was significantly increased in the $ER\alpha^{-/NERKI}$, but not in the $ER\alpha^{+/NERKI}$, compared with the $ER\alpha^{+/+}$ mice. As is evi-

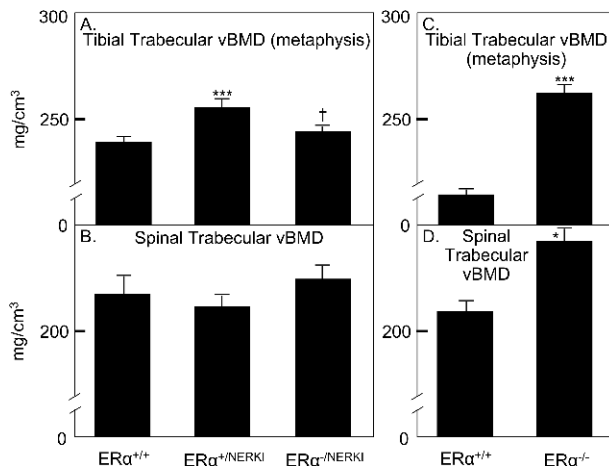


FIG. 2. Baseline trabecular vBMD as measured by pQCT at (A and C) the proximal tibial metaphysis ($n = 46\text{--}48/\text{genotype}$) and (B and D) lumbar spine vBMD measured ex vivo in 5-month-old sham-operated mice ($n = 10\text{--}12/\text{genotype}$). $***p < 0.001$ vs. the respective $ER\alpha^{+/+}$ and $†p < 0.05$ vs. $ER\alpha^{+/NERKI}$ mice.

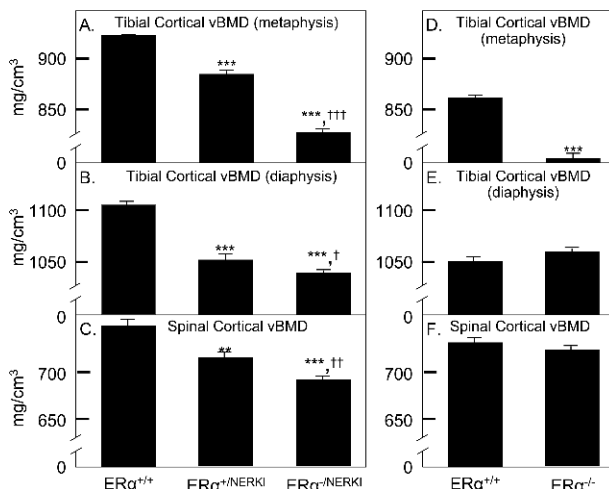


FIG. 3. Baseline cortical vBMD as measured by pQCT at (A and D) the proximal tibial metaphysis ($n = 46\text{--}48/\text{genotype}$), (B and E) diaphysis ($n = 46\text{--}48/\text{genotype}$), and (C and F) lumbar spine cortical vBMD measured ex vivo in 5-month-old sham-operated mice ($n = 10\text{--}12/\text{genotype}$). $***p < 0.001$, $**p < 0.01$ vs. the respective $ER\alpha^{+/+}$ and $†††p < 0.001$, $††p < 0.01$, $†p < 0.05$ vs. $ER\alpha^{+/NERKI}$ mice.

dent from Table 1, all of the cortical deficits were much more severe in the $ER\alpha^{-/NERKI}$ compared with the $ER\alpha^{+/NERKI}$ mice. Finally, the $ER\alpha^{-/-}$ mice had decreased cortical vBMD at the tibial metaphysis (Fig. 3D), but not at the diaphysis (Fig. 3E) or lumbar spine (Fig. 3F).

Response to OVX and E replacement

Because changes in circulating serum E_2 levels could account, at least in part, for the observed skeletal changes in the genotypes studied, these were also assessed in a subset of four to five mice per genotype at 3 months of age. The $ER\alpha^{+/NERKI}$ (26.5 ± 5.1 pM) had similar serum E_2 levels

TABLE 1. BASELINE CORTICAL PARAMETERS AT THE TIBIAL METAPHYSIS AND DIAPHYSIS AS ASSESSED BY pQCT (N = 46–48 GENOTYPE)

Parameter	ER $\alpha^{+/+}$	ER $\alpha^{+/NERKI}$	ER $\alpha^{-/NERKI}$
Cortical area (mm ²)			
Metaphysis	1.23 \pm 0.027	0.97 \pm 0.027†	0.42 \pm 0.015†¶
Diaphysis	0.79 \pm 0.008	0.70 \pm 0.008†	0.67 \pm 0.008†§
Cortical thickness (mm)			
Metaphysis	0.20 \pm 0.004	0.16 \pm 0.005†	0.07 \pm 0.003†¶
Diaphysis	0.22 \pm 0.002	0.20 \pm 0.002†	0.19 \pm 0.002†¶
Endocortical circumference (mm)			
Metaphysis	5.66 \pm 0.051	5.59 \pm 0.052	5.92 \pm 0.049†¶
Diaphysis	2.86 \pm 0.017	2.91 \pm 0.022	2.96 \pm 0.016†‡
Periosteal circumference (mm)			
Metaphysis	6.89 \pm 0.045	6.59 \pm 0.041†	6.35 \pm 0.038†¶
Diaphysis	4.25 \pm 0.018	3.14 \pm 0.022*	4.14 \pm 0.019†

* p < 0.01, †p < 0.001 vs. ER $\alpha^{+/+}$

‡ p < 0.05, §p < 0.01, ¶p < 0.001 vs. ER $\alpha^{+/NERKI}$.

relative to their ER $\alpha^{+/+}$ controls (27.2 \pm 3.9 pM). As such, the deficit in cortical vBMD in the ER $\alpha^{+/NERKI}$ mice could not be accounted for by alterations in circulating E₂ levels. However, the ER $\alpha^{-/NERKI}$ mice did have significantly elevated E₂ levels (52.0 \pm 6.8 pM; p < 0.05 versus the ER $\alpha^{+/+}$ mice). Thus, to evaluate whether these altered E₂ levels accounted for at least part of the skeletal changes in the ER $\alpha^{-/NERKI}$ mice, we next compared the effects of OVX followed by fixed doses of E₂ replacement in these mice. Moreover, to test whether any alterations in the response to E were caused by potentially unique actions of the NERKI receptor, we also placed the changes in the ER $\alpha^{-/NERKI}$ versus their control ER $\alpha^{+/+}$ mice in the context of changes in the ER $\alpha^{-/}$ versus their corresponding control ER $\alpha^{+/+}$ mice.

Effects of OVX and E replacement on trabecular bone: To evaluate the effects of OVX and E replacement on trabecular bone, we first assessed changes in trabecular vBMD at the tibial metaphysis (Table 2). The ER $\alpha^{+/+}$ controls as well as ER $\alpha^{+/NERKI}$, ER $\alpha^{-/NERKI}$, and ER $\alpha^{-/}$ lost bone at this site after OVX. E replacement did prevent OVX-induced bone loss in the ER $\alpha^{-/NERKI}$ (at least at the lower dose), whereas neither dose of E was effective in the ER $\alpha^{-/}$ mice. The overall pattern of changes was qualitatively similar to the ER $\alpha^{+/+}$ mice in the ER $\alpha^{+/NERKI}$ mice, although the increase in vBMD present at the higher dose of E in the ER $\alpha^{+/+}$ mice was attenuated in the ER $\alpha^{+/NERKI}$ mice. Figure 4 provides a visual demonstration, using μ CT, of the pattern of changes in trabecular bone in the femur metaphysis in the ER $\alpha^{+/+}$ and the ER $\alpha^{-/NERKI}$ mice, with the latter responding to E with a preservation of trabecular bone but lacking the marked increase in trabecular bone present in the ER $\alpha^{+/+}$ mice at the higher dose of E. Changes in trabecular bone in the spine were also assessed by histomorphometry in the ER $\alpha^{+/+}$ and ER $\alpha^{-/NERKI}$ mice (Table 2). Similar to trabecular bone at the tibia, E was effective in preventing OVX-induced bone loss at the spine in the ER $\alpha^{-/NERKI}$ mice, although the response to E was clearly attenuated compared with the ER $\alpha^{+/+}$ mice.

Paradoxical responses to OVX and E replacement in cor-

tical bone of ER $\alpha^{-/NERKI}$ mice: Figure 5 shows the corresponding changes in tibial cortical vBMD at the metaphysis (Figs. 5A and 5B) and diaphysis (Figs. 5C and 5D). Strikingly, the pattern of changes in tibial cortical vBMD at both sites was the exact opposite in the ER $\alpha^{-/NERKI}$ compared with the ER $\alpha^{+/+}$ mice. Thus, relative to the sham mice, the ER $\alpha^{-/NERKI}$ mice gained more bone (not less, as in the ER $\alpha^{+/+}$ mice) and E dose-dependently suppressed this increase (Figs. 5A and 5C). In contrast, E enhanced increases in cortical vBMD at both the tibial metaphysis and diaphysis in the ER $\alpha^{+/+}$ mice. The paradoxical increase in cortical vBMD in the ER $\alpha^{-/NERKI}$ mice after OVX was distinctly different from the changes observed in the ER $\alpha^{-/}$ mice (Figs. 5B and 5D); specifically, in contrast to the findings in the ER $\alpha^{-/NERKI}$ mice, there was no increase in cortical vBMD after OVX at either the tibial metaphysis or diaphysis in the ER $\alpha^{-/}$ mice. In fact, cortical vBMD at both sites was essentially unresponsive to OVX or E replacement in the ER $\alpha^{-/}$ mice. The only exception was the high dose of E, which did result in an inhibitory effect on cortical vBMD at the diaphysis in the ER $\alpha^{-/}$ mice. The ER $\alpha^{+/NERKI}$ mice showed essentially the same pattern of changes in cortical vBMD at both sites as the ER $\alpha^{+/+}$ mice, although the response to E at the higher dose was attenuated (Figs. 5A and 5C).

Effects of OVX and E replacement on aBMD at the femur and spine: The femur typifies the appendicular skeleton and contains predominantly cortical bone, but there is also a significant amount of trabecular bone in the femur metaphyses. In an analogous fashion, the lumbar vertebrae are representative of the axial skeleton and predominantly consist of trabecular bone, but they are also enclosed in a cortical rim and have posterior elements that are composed of cortical bone. Based on the observed distinct changes in trabecular and cortical bone in the ER $\alpha^{-/NERKI}$ relative to their wildtype control mice described above, one would expect that the patterns seen in aBMD by DXA at the femur and spine after OVX or E replacement would reflect a summation of responses in the respective trabecular and cortical compartments. That this was, indeed, the case, is shown in Fig. 6, which depicts the percent change from baseline in the femur and spine aBMDs by DXA after the various treatments in the genotypes studied. Changes in femur aBMD were significantly different after OVX in all groups compared with the sham mice. The 0.25 μ g/day dose of E was effective in preventing bone loss at the femur in the ER $\alpha^{+/+}$ and the ER $\alpha^{+/NERKI}$ mice; however, at the 1.0 μ g/day dose, increases in femur aBMD were not as large in the ER $\alpha^{+/NERKI}$ mice. In contrast, in the ER $\alpha^{-/NERKI}$ mice, the lower dose of 0.25 μ g/day was not effective in preventing bone loss and the higher dose of 1.0 μ g/day even resulted in a further decrease in aBMD relative to the sham mice. Whereas the ER $\alpha^{-/}$ mice lost bone at the femur after OVX, neither dose of E used was effective in preventing this bone loss (Fig. 6B). An overall similar pattern of changes was seen at the spine in all the genotypes, except that in the ER $\alpha^{-/}$ mice, the high dose exhibited a trend toward preventing bone loss at the spine (Fig. 6D). Based on the findings previously noted using pQCT, which showed a suppression of cortical vBMD by E in the

TABLE 2. PERCENT CHANGES FROM BASELINE IN TIBIAL TRABECULAR vBMD AT THE METAPHYSIS AS ASSESSED BY pQCT IN THE ER $\alpha^{+/NERKI}$, ER $\alpha^{-/NERKI}$, AND ER $\alpha^{-/-}$ MICE VS. THEIR RESPECTIVE CONTROL ER $\alpha^{+/+}$ MICE (N = 10–12/GROUP) AND IN LUMBAR SPINE %BV/TV (N = 9–10/GROUP) AS ASSESSED BY HISTOMORPHOMETRY IN THE ER $\alpha^{-/NERKI}$ MICE VS. CONTROL ER $\alpha^{+/+}$ MICE AFTER DIFFERENT TREATMENTS

Genotype	Sham	OVX	OVX + E _{0.25}	OVX + E _{1.0}
Tibial trabecular BMD (% change)				
ER $\alpha^{+/+}$	-14.2 ± 1.8‡	-31.2 ± 2.3	49.8 ± 27.1†	169 ± 23.9‡
ER $\alpha^{+/NERKI}$	-12.3 ± 1.4‡	-26.5 ± 1.9	36.1 ± 18.6†	45.5 ± 15.1‡
ER $\alpha^{-/NERKI}$	-9.34 ± 1.4‡	-25.0 ± 1.4	-8.9 ± 6.7*	-21.2 ± 2.1
ER $\alpha^{+/+}$	-14 ± 1.36†	-25.5 ± 3.1	43.4 ± 26.9*	68.6 ± 21.2‡
ER $\alpha^{-/-}$	-7.58 ± 1.84‡	-36.4 ± 2.7	-30.7 ± 5.5	-34.0 ± 1.7
Lumbar spine (%BV/TV)				
ER $\alpha^{+/+}$	21.2 ± 4.0‡	10.8 ± 3.9	27.1 ± 10.3‡	36.0 ± 8.1‡
ER $\alpha^{-/NERKI}$	18.4 ± 2.0‡	7.4 ± 2.5	16.1 ± 5.6‡	18.1 ± 4.5‡

Overall p for genotype vs. treatment interaction for the percent change in tibial trabecular vBMD was <0.001 for the ER $\alpha^{+/NERKI}$, ER $\alpha^{-/NERKI}$, and ER $\alpha^{-/-}$ mice vs. the respective ER $\alpha^{+/+}$ controls and <0.0001 for BV/TV in the ER $\alpha^{-/NERKI}$ vs. the ER $\alpha^{+/+}$ controls.

* p < 0.05, †p < 0.01, and ‡p < 0.001 vs. the OVX group within each genotype.

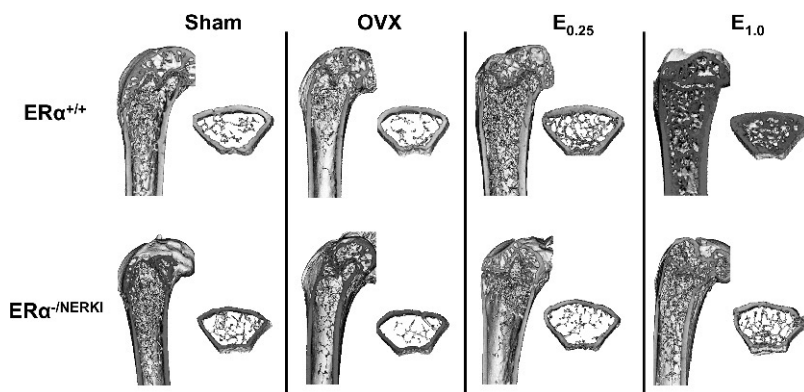


FIG. 4. μ CT analysis at an 11- μ m resolution of the proximal femur metaphysis in the ER $\alpha^{+/+}$ and ER $\alpha^{-/NERKI}$ mice after the various treatments. (Left) Sagittal section. (Right) Cross-section through the metaphysis. Evident in these representative scans is the loss of trabecular bone after OVX in both groups, with a preservation of trabecular bone in the ER $\alpha^{+/+}$ and ER $\alpha^{-/NERKI}$ mice with E replacement. However, the marked increase in trabecular bone present in the ER $\alpha^{+/+}$ mice after the higher dose of E is not present in the ER $\alpha^{-/NERKI}$ mice.

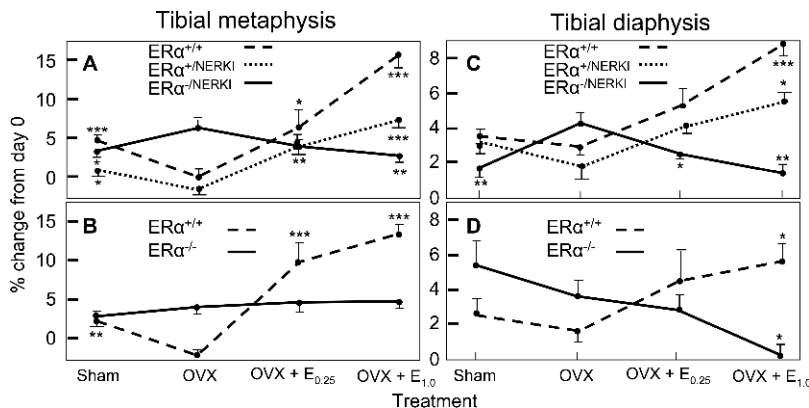


FIG. 5. Changes in cortical vBMD at the (A and B) tibial metaphysis and (C and D) diaphysis in the (A and C) ER $\alpha^{+/+NERKI}$ and ER $\alpha^{-/NERKI}$ and (B and D) ER $\alpha^{-/-}$ mice relative to their respective ER $\alpha^{+/+}$ controls (n = 10–12/group). Overall p value for a genotype vs. treatment interaction was 0.03 for the ER $\alpha^{+/+NERKI}$ and <0.0001 for ER $\alpha^{-/NERKI}$ and ER $\alpha^{-/-}$ vs. their respective ER $\alpha^{+/+}$ controls at the metaphysis and 0.23 for ER $\alpha^{+/+NERKI}$, <0.0001 for ER $\alpha^{-/NERKI}$, and 0.002 for ER $\alpha^{-/-}$ vs. their respective ER $\alpha^{+/+}$ controls at the diaphysis. *p < 0.05, **p < 0.01, ***p < 0.001 vs. the OVX group within each genotype. In B, the asterisks in the sham are for the difference in the ER $\alpha^{+/+}$ sham vs. OVX mice.

ER $\alpha^{-/NERKI}$ mice, the observed decrease in aBMD in the ER $\alpha^{-/NERKI}$ mice at the femur and spine after high-dose E treatment is likely caused by the effects of E on the cortical compartments at these sites.

Changes in endocortical MARs and eroded surfaces: It should also be noted that, in addition to the paradoxical responses observed in cortical bone (Fig. 5), the ER $\alpha^{-/NERKI}$ mice had a greater endocortical circumference at baseline both at the metaphysis and diaphysis (Table 1), suggesting that E may inhibit endocortical bone formation

and/or stimulate endocortical bone resorption in these mice. Thus, to further explore these unexpected findings in cortical bone, we first assessed endocortical MARs in the ER $\alpha^{-/NERKI}$ and ER $\alpha^{-/-}$ as well as their respective wildtype control mice. A similar, paradoxical response to OVX and E treatment was evident for changes in endocortical MAR, an index of osteoblastic activity, in the ER $\alpha^{-/NERKI}$ mice (Fig. 7A). Thus, in the ER $\alpha^{+/+}$ mice, endocortical MAR decreased after OVX, with E treatment clearly increasing MAR. In contrast, in the ER $\alpha^{-/NERKI}$ mice, endocortical

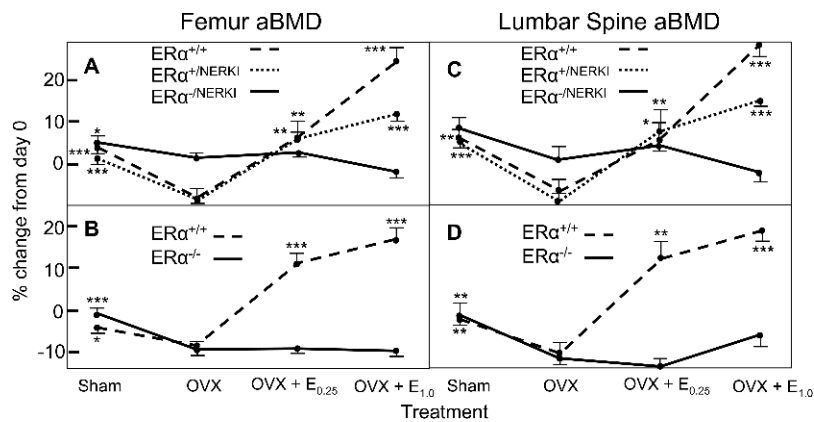


FIG. 6. Changes in (A and B) femur and (C and D) lumbar spine aBMD as measured by DXA in the (A and C) ERα^{-/-} and ERα^{+/-} mice relative to their respective ERα^{+/+} controls ($n = 10-12$ /group). Overall p value for a genotype vs. treatment interaction was 0.06 for ERα^{+/-} and <0.0001 for ERα^{-/-} and ERα^{+/-} vs. their respective ERα^{+/+} controls at the femur and 0.11 for ERα^{+/-} and <0.0001 for ERα^{-/-} and ERα^{+/-} vs. their respective ERα^{+/+} controls at the lumbar spine. * $p < 0.05$, ** $p < 0.01$, *** $p < 0.001$ vs. the OVX group within each genotype.

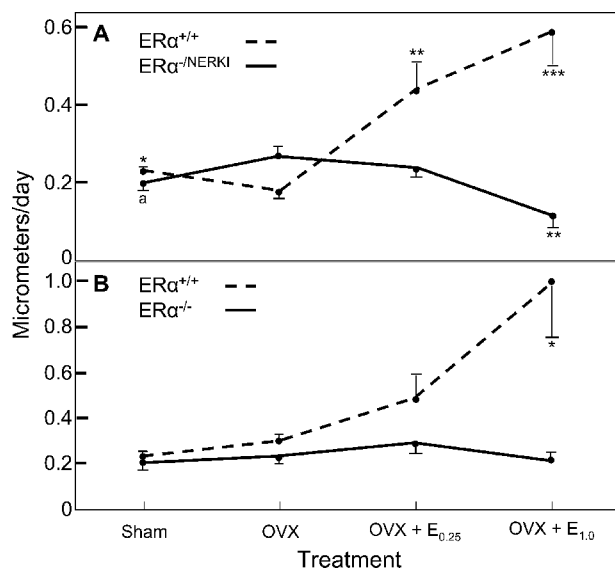


FIG. 7. Changes in endocortical MAR in (A) ERα^{-/-} and (B) ERα^{+/+} relative to their respective ERα^{+/+} controls ($n = 10-12$ /group). Overall p value for a genotype vs. treatment interaction was <0.0001 for ERα^{-/-} and 0.002 for ERα^{+/+} vs. their respective ERα^{+/+} controls. ^a $p = 0.07$, * $p < 0.05$, ** $p < 0.01$, *** $p < 0.001$ vs. the OVX group within each genotype.

MAR tended to increase after OVX, with E treatment resulting in a suppression of MAR on the endocortical surface. Again, this pattern of changes in the ERα^{-/-} mice was distinctly different from that observed in the ERα^{+/+} mice relative to their controls (Fig. 7B). Whereas E increased endocortical MARs in the ERα^{+/+} mice, MARs were entirely insensitive to OVX or E replacement in the ERα^{-/-} mice. Combined with the changes in cortical vBMD shown in Fig. 5, these data show that the ERα^{-/-} had a pattern of changes in cortical bone parameters after OVX and E replacement that was distinct not only from the ERα^{+/+} and ERα^{+/-} mice, but also compared with the changes observed in the ERα^{-/-} mice. Note that, whereas the ERα^{+/+} mice in the 50:50 C57BL/6:129SvJ background had a decrease in endocortical MAR after OVX (Fig. 7A), this was not present in the ERα^{+/+} mice in the complete

C57BL/6 background (Fig. 7B). Whether this was caused by strain differences or to chance is unclear.

We also examined changes in percent eroded surface, an index of osteoclastic activity, in cortical bone in the ERα^{-/-} mice relative to their ERα^{+/+} controls. As expected, percent eroded surface increased after OVX in the ERα^{+/+} mice (sham, $3.8 \pm 1.4\%$, OVX, $8.0 \pm 1.1\%$; $p < 0.05$). In contrast, percent eroded surface showed the exact opposite pattern in the ERα^{-/-} mice, that is, it decreased after OVX (sham, $4.6 \pm 1.1\%$, OVX, $1.6 \pm 0.4\%$; $p < 0.05$), and in both groups, E reversed these changes (for E_{0.25}, to $4.3 \pm 0.8\%$ in the ERα^{+/+} and to $4.7 \pm 1.1\%$ in the ERα^{-/-} mice, $p =$ not significant for both compared with their respective sham groups).

Changes in circulating IGF-I levels: Because the apparent paradoxical changes in cortical vBMD and in endocortical MARs could be caused by a different pattern of changes in circulating IGF-I levels in the ERα^{+/+} versus the ERα^{-/-} mice, we also measured serum IGF-I levels in the two groups (Table 3). Whereas serum IGF-I levels were lower in the sham ERα^{-/-} mice compared with the ERα^{+/+} mice, IGF-I levels increased similarly after OVX in both groups and returned to baseline with E treatment (Table 3). Thus, the paradoxical changes in cortical vBMD and endocortical MARs in the ERα^{-/-} mice could not be explained by differing changes in serum IGF-I levels after OVX and E replacement in the ERα^{+/+} compared with the ERα^{-/-} mice.

Changes in uterine weights: Uterine wet weights were measured at the time of death to assess the efficacy of OVX and E replacement and to characterize the uterine response to these interventions in the various groups. As shown in Table 4, both the ERα^{-/-} and ERα^{+/+} mice had reduced uterine weights compared with their respective ERα^{+/+} controls under sham conditions. Moreover, both groups of mice had a decrease in uterine weight after OVX. However, whereas E partially restored uterine weight to baseline in the ERα^{-/-} mice, it was entirely ineffective (even at the higher dose) in the ERα^{+/+} mice. The ERα^{+/+} mice have previously been found to have an increase in uterine weight under basal conditions and a supranormal response to E treatment,⁽¹⁹⁾ and we also found this to be the case (Table 4).

TABLE 3. SERUM IGF-I LEVELS (ng/ml) IN THE ER $\alpha^{+/+}$ AND ER $\alpha^{-/NERKI}$ MICE AFTER THE VARIOUS TREATMENTS (N = 10–12 GROUP)

	Sham	OVX + V	OVX + E _{0.25}	OVX + E _{1.0}
ER $\alpha^{+/+}$	217 ± 13*	254 ± 8	260 ± 11	221 ± 11
ER $\alpha^{-/NERKI}$	164 ± 6‡	212 ± 7	207 ± 12	172 ± 9†

Overall p for genotype vs. treatment interaction was 0.933 for the ER $\alpha^{-/NERKI}$ vs. the ER $\alpha^{+/+}$ controls.

* p < 0.05, †p < 0.01, and ‡p < 0.001 vs. the OVX group within each genotype.

TABLE 4. CHANGES IN UTERINE WEIGHT (mg) IN THE ER $\alpha^{+/NERKI}$, ER $\alpha^{-/NERKI}$, AND ER $\alpha^{-/-}$ RELATIVE TO THEIR RESPECTIVE ER $\alpha^{+/+}$ CONTROLS (N = 10–12/GROUP)

	Sham	OVX + V	OVX + E _{0.25}	OVX + E _{1.0}
ER $\alpha^{+/+}$	145 ± 12‡	55 ± 4	83 ± 18	163 ± 24‡
ER $\alpha^{+/NERKI}$	300 ± 21‡	88 ± 10	321 ± 81†	391 ± 45‡
ER $\alpha^{-/NERKI}$	78 ± 4‡	46 ± 5	63 ± 5*	55 ± 4
ER $\alpha^{+/+}$	100 ± 7‡	40 ± 3	70 ± 13*	110 ± 12‡
ER $\alpha^{-/-}$	70 ± 7‡	30 ± 3	40 ± 7	40 ± 7

Overall p for a genotype vs. treatment interaction was 0.011 for the ER $\alpha^{+/NERKI}$, <0.001 for the ER $\alpha^{-/NERKI}$, and 0.012 for the ER $\alpha^{-/-}$ vs. their respective ER $\alpha^{+/+}$ controls.

* p < 0.05, †p < 0.01, and ‡p < 0.001 vs. the OVX group within each genotype.

DISCUSSION

In this study, we generated mice (ER $\alpha^{-/NERKI}$) in whom ER α could signal only through non-ERE (or nonclassical) pathways. Whereas these mice have preserved trabecular vBMD at the tibia and spine under basal conditions, they clearly have attenuated responses to E in trabecular bone. In contrast to trabecular vBMD, cortical vBMD is reduced at multiple sites in the ER $\alpha^{-/NERKI}$ mice. Moreover, the most striking finding in these mice is the apparent paradoxical response of cortical bone to OVX and E replacement as assessed by cortical vBMD, endocortical MAR, and resorption indices. This pattern is distinctly different from that seen in the ER $\alpha^{-/-}$ mice, indicating that the observed skeletal changes in the ER $\alpha^{-/NERKI}$ are caused by unique actions of the NERKI receptor. Specifically, because both the ER $\alpha^{-/NERKI}$ and ER $\alpha^{-/-}$ mice have intact ER β signaling, the divergence of responses in cortical bone between the two genotypes effectively excludes the possibility that the findings in the ER $\alpha^{-/NERKI}$ mice are mediated by ER β and therefore must be due, instead, to direct actions of the NERKI receptor.

As noted earlier, the initial phenotyping of reproductive tissues in the heterozygote female NERKI mice showed significant ovarian and uterine abnormalities.⁽¹⁹⁾ Thus, these mice had no corpora lutea in the ovaries, displayed altered steroidogenesis, and had abnormally large uteri with evidence of cystic endometrial hyperplasia.⁽¹⁹⁾ The NERKI receptor was also found not to be a dominant negative receptor for ER α ,⁽¹⁹⁾ and the authors suggested that the reproductive abnormalities in the heterozygote NERKI

female mice may be caused by an altered balance between classical and nonclassical ER α signaling pathways. We believe our findings provide further support for this hypothesis and, in fact, indicate that this altered balance in the ER $\alpha^{-/NERKI}$ mice leads to the paradoxical effects of OVX and E replacement in cortical bone in these mice.

In the ER $\alpha^{+/+}$ mice, OVX led to a reduction in endocortical MAR, an increase in resorption surfaces, and a reduction in cortical vBMD relative to the sham mice; these changes were prevented by E replacement. Thus, E was important in maintaining bone formation, inhibiting bone resorption, and preserving cortical vBMD in these mice. In contrast, in the ER $\alpha^{-/NERKI}$ mice, OVX resulted in a rise in MAR, a decrease in resorption surfaces, and an increase in cortical vBMD relative to the sham mice, and E reversed these changes. Collectively, these findings suggest that classical signaling through EREs activates pathways in osteoblasts (and perhaps osteoclasts) that are important for the maintenance of bone formation and suppression of bone resorption. Loss of classical ERE signaling apparently leads to an altered balance of classical versus nonclassical signaling, with E now suppressing bone formation and stimulating bone resorption in the ER $\alpha^{-/NERKI}$ mice. Thus, our findings clearly establish a phenotype of an aberrant skeletal response to E in the ER $\alpha^{-/NERKI}$ mice. Whereas one could speculate on the particular pathways involved in mediating this aberrant response to E (e.g., increased AP-1 activity), further studies using gene array or proteomic analyses of the bones and/or cells derived from ER $\alpha^{+/+}$ versus ER $\alpha^{-/NERKI}$ mice are needed to define the specific pathways activated (or suppressed) by nonclassical ER α signaling that lead to the paradoxical responses to E in cortical bone in the ER $\alpha^{-/NERKI}$ mice.

ER $\alpha^{-/NERKI}$ mice did have reduced serum IGF-I levels compared with their ER $\alpha^{+/+}$ controls. Because IGF-I is an important skeletal growth factor, particularly for cortical bone,⁽²⁵⁾ the baseline deficits in bone size and in cortical vBMD in the ER $\alpha^{-/NERKI}$ mice could be caused by impaired IGF-I production either in the liver or possibly in bone. However, after OVX and E replacement, the pattern of changes in serum IGF-I were identical in the ER $\alpha^{-/NERKI}$ and ER $\alpha^{+/+}$ control mice, providing strong evidence that the aberrant cortical response to OVX and E replacement in the ER $\alpha^{-/NERKI}$ mice was likely caused by an intrinsic skeletal abnormality in E action in these mice and not divergent changes in IGF-I production in the ER $\alpha^{-/NERKI}$ versus the ER $\alpha^{+/+}$ mice. We acknowledge, however, that we cannot exclude the possibility that at least part of the aberrant response to E in the ER $\alpha^{-/NERKI}$ may be caused by secondary changes in other hormones or growth factors that we did not measure. This is an inherent limitation of these types of in vivo studies.

It is also of note that the paradoxical responses to OVX and E replacement in the ER $\alpha^{-/NERKI}$ mice were present in cortical, but not in trabecular, bone. Previous studies by us⁽⁷⁾ and others^(5,6) have shown that cortical bone predominantly contains ER α with little or no ER β . In contrast, trabecular bone contains both receptors, with ER β perhaps expressed at higher levels.^(5–7) As such, it is not surprising that the most significant findings in the ER $\alpha^{-/NERKI}$ mice

(which have a knock-in mutation in the *ERα* gene) are in cortical bone: the NERKI receptor is likely expressed at higher levels in cortical bone and is largely unopposed there by *ERβ*.

Whereas trabecular bone did not show an abnormal pattern of changes after OVX and E replacement in the *ERα^{-NERKI}* mice, the response to E was clearly attenuated in trabecular bone in these mice. Specifically, E replacement (particularly at the higher dose) resulted in a significant increase in BMD and bone volume in the *ERα^{+/+}* mice, which was absent in the *ERα^{-NERKI}* mice. This osteogenic effect of E has been previously observed in trabecular bone in mice⁽²⁶⁾ and is absent in *ERα^{-/-}* mice.⁽²⁷⁾ Our findings indicate that not only is *ERα* necessary for the osteogenic response to E in trabecular bone but that classical ERE signaling and/or the balance between classical and nonclassical signaling pathways may also be critical. Moreover, it is of interest that a recent study⁽²⁸⁾ found that E activated BMP2 gene transcription in mouse mesenchymal cells and that the BMP2 promoter contains a sequence that resembles the classical ERE. Thus, whether part of the anabolic effect of E on bone is caused by an ERE-mediated increase in osteoblastic BMP2 production is an intriguing question that warrants further study.

Whereas the *ERα^{+NERKI}* mice, which possess both a wildtype and NERKI receptor, did not exhibit paradoxical responses to E in cortical bone, effects of E were attenuated in both trabecular and cortical bone in these mice. Moreover, the *ERα^{+NERKI}* mice also had reduced cortical vBMD and thickness under basal conditions, although these deficits were not as severe as those present in the *ERα^{-NERKI}* mice. These findings provide further support for the hypothesis that the balance of classical versus nonclassical *ERα* signaling is important, particularly in cortical bone. Thus, in the *ERα^{+NERKI}* mice, both pathways are active, but the nonclassical pathway is likely enhanced compared with wildtype mice.

It is also useful to place the skeletal phenotype of the *ERα^{-NERKI}* mice in the context of findings of other groups in mice with deletion of *ERα*. *ERα^{-/-}* mice have been generated independently by two groups,^(21,29) and their skeletal phenotypes were characterized. Lindberg et al.⁽³⁰⁾ showed that 2- to 4-month-old *ERα^{-/-}* mice had increased cortical and trabecular bone parameters compared with wildtype mice. It should, however, be noted that these mice expressed a splice variant of *ERα*.⁽³¹⁾ On the other hand, Sims et al.,⁽⁴⁾ using complete *ERα* knockout mice, have shown that loss of *ERα* leads to increased trabecular bone volume and decreased cortical density in both sexes. As is evident from the baseline data presented here (Figs. 1–3), the *ERα^{-NERKI}* mice are similar to *ERα^{-/-}* mice in that they display reduced cortical bone parameters, with the deficit being clearly more pronounced in the *ERα^{-NERKI}* mice. Furthermore, in contrast to *ERα^{-/-}* mice, which exhibit significantly increased trabecular vBMD both at the tibial metaphysis and lumbar spine, the *ERα^{-NERKI}* mice have similar trabecular vBMD at these sites as their wildtype littermates. In another report, Sims et al.⁽³⁾ showed that *ERα^{-/-}* mice were partially protected against OVX-induced bone loss by E, indicating that *ERβ* could compen-

sate for lack of *ERα* on bone turnover parameters, at least in female mice. Our results with the *ERα^{-NERKI}* mice indicate that classical ERE signaling is essential for maintenance of cortical bone and its normal response to OVX and E replacement. In contrast, it seems that a compensatory *ERβ* mechanism may well play a role in trabecular bone in *ERα^{-NERKI}* mice, because similar to *ERα^{-/-}* mice, *ERα^{-NERKI}* mice do have at least an attenuated response to E in trabecular bone.

Although the classical *ERα* signaling pathway has been well characterized at the molecular level, nonclassical *ERα* signaling pathways are less well understood. A number of studies have recently been carried out in vitro to understand the molecular basis of *ERα* action at AP-1 sites.^(20,32) Recently, Cheung et al.⁽³³⁾ have described altered pharmacology and distinct coactivator use by *ERα*-dependent pathways at AP-1 compared with ERE sites using an in vitro assay, further adding to the increasing complexity of *ER* signaling pathways. The exact mechanisms of *ERα* actions at AP-1 sites (or other sites involving *ER* interactions with various proteins) with agonists and antagonists, however, remains a topic of debate, with different studies describing varying results in vitro,^(13,33) underscoring the need for further work.

In summary, our studies on the skeletal phenotype of the *ERα^{-NERKI}* mice represent the first demonstration, in any tissue, that complete loss of classical ERE signaling can lead to a paradoxical response to E. These data strongly support the hypothesis that in bone, and perhaps in other tissues, there exists a balance between classical and nonclassical *ERα* signaling pathways. Alteration of this balance solely toward nonclassical pathways can result in a markedly aberrant response to E. Defining the molecular mechanisms responsible for these changes in the *ERα^{-NERKI}* mice should provide novel insights into the specific mediators of E action on bone through these pathways.

ACKNOWLEDGMENTS

We thank David Nagel for performing the sectioning and histomorphometry of the mouse bones, Dr Jean Sibonga for technical advice regarding the bone histomorphometry, Jesse Lamsam and Kelley Hoey for technical assistance, James Peterson for help with the statistical analyses and preparation of the figures, and Dr Erik L. Ritman and Patricia E. Beighley for performing the μ CT analyses. This study was supported by NIH Grants P01 AG004875 (TCS and SK) and HD21921 (JLJ).

REFERENCES

1. Riggs BL, Khosla S, Melton LJ 2002 Sex steroids and the construction and conservation of the adult skeleton. *Endocr Rev* 23:279–302.
2. Spelsberg TC, Subramaniam M, Riggs BL, Khosla S 1999 The actions and interactions of sex steroids and growth factors/cytokines on the skeleton. *Mol Endocrinol* 13:819–828.
3. Sims NA, Clement-Lacroix P, Minet D, Fraslon-Vanhulle C, Gaillard-Kelly M, Resche-Rigon M, Baron R 2003 A functional androgen receptor is not sufficient to allow estradiol to protect bone after gonadectomy in estradiol receptor-deficient mice. *J Clin Invest* 111:1319–1327.

4. Sims NA, Dupont S, Krust A, Clement-LaCroix P, Minet D, Resche-Rigon M, Gaillard-Kelly M, Baron R 2002 Deletion of estrogen receptors reveals a regulatory role for estrogen receptors beta in bone remodeling in females but not in males. *Bone* **30**:18–25.
5. Bord S, Horner A, Beavan S, Compston J 2001 Estrogen receptors alpha and beta are differentially expressed in developing human bone. *J Clin Endocrinol Metab* **86**:2309–2314.
6. Onoe Y, Miyaura C, Ohta H, Nozawa S, Suda T 1997 Expression of estrogen receptor beta in rat bone. *Endocrinology* **138**:4509–4512.
7. Modder UJL, Sanyal A, Kearns AE, Sibonga JD, Nishihara E, Xu J, O'Malley BW, Ritman EL, Riggs BL, Spelsberg TC, Khosla S 2004 Effects of loss of steroid receptor coactivator-1 on the skeletal response to estrogen in mice. *Endocrinology* **145**:913–921.
8. Hall JM, McDonnell DP 1999 The estrogen receptor beta-isoform (ER-beta) of the human estrogen receptor modulates ER-alpha transcriptional activity and is a key regulator of the cellular response to estrogens and antiestrogens. *Endocrinology* **140**:5566–5578.
9. Beato M, Herrlich P, Schutz G 1995 Steroid hormone receptors: Many actors in search of a plot. *Cell* **83**:851–857.
10. Maurer RA, Notides AC 1987 Identification of an estrogen-responsive element from the 5'-flanking region of the rat prolactin gene. *Mol Cell Biol* **7**:4247–4254.
11. Savouret J-F, Bailly A, Misrahi M, Rauch C, Redeuilh G, Chachereau A, Milgrom E 1991 Characterization of the hormone responsive element involved in the regulation of the progesterone receptor gene. *EMBO J* **10**:1875–1883.
12. Weisz A, Rosales R 1990 Identification of an estrogen response element upstream of the human c-fos gene that binds the estrogen receptor and the AP-1 transcription factor. *Nucleic Acids Res* **18**:5097–5106.
13. Paech K, Webb P, Kuiper GGJM, Nilsson S, Gustafsson JA, Kushner PJ, Scanlan TS 1997 Differential ligand activation of estrogen receptors ERalpha and ERbeta at AP1 sites. *Science* **277**:1508–1510.
14. Umayahara Y, Kawamori R, Watada H, Imano E, Iwama N, Morishima T, Yamasaki Y, Kajimoto Y, Kamada T 1994 Estrogen regulation of the insulin-like growth factor I gene transcription involves an AP-1 enhancer. *J Biol Chem* **269**:16433–16441.
15. Ray A, Prefontaine KE, Ray P 1994 Down-modulation of interleukin-6 gene expression by 17beta-estradiol in the absence of high affinity DNA binding by the estrogen receptor. *J Biol Chem* **269**:12940–12946.
16. Chang LC, Karen M 2001 Mammalian MAP kinase signalling cascades. *Nature* **410**:37–40.
17. Kousteni S, Bellido T, Plotkin LI, O'Brien CA, Bodenner DL, Han L, Han K, DiGregorio GB, Katzenellenbogen JA, Katzenellenbogen BS, Roberson PK, Weinstein RS, Jilka RL, Manolagas SC 2001 Nongenotropic, sex-nonspecific signaling through the estrogen or androgen receptors: Dissociation from transcriptional activity. *Cell* **104**:1–20.
18. Manolagas SC, Kousteni S 2001 Perspective: Nonreproductive sites of action of reproductive hormones. *Endocrinology* **142**:2200–2204.
19. Jakacka M, Ito M, Martinson F, Ishikawa T, Lee EJ, Jameson JL 2002 An estrogen receptor (ER)alpha deoxyribonucleic acid-binding domain knock-in mutation provides evidence for nonclassical ER pathway signaling in vivo. *Mol Endocrinol* **16**:2188–2201.
20. Jakacka M, Ito M, Weiss J, Chien P-Y, Gehm BD, Jameson JL 2001 Estrogen receptor binding to DNA is not required for its activity through the nonclassical AP1 pathway. *J Biol Chem* **276**:13615–13621.
21. Dupont S, Krust A, Gansmuller A, Dierich A, Chambon P, Mark M 2000 Effect of single and compound knockouts of estrogen receptors alpha (ERalpha) and beta (ERbeta) on mouse reproductive phenotypes. *Development* **127**:4277–4291.
22. Eckstein F, Pavicic T, Nedbal S, Schmidt C, Wahr U, Rambeck W, Wolf E, Hoefflich A 2002 Insulin-like growth factor-binding protein-2 (IGFBP-2) overexpression negatively regulates bone size and mass, but not density, in the absence and presence of growth hormone/IGF-I excess in transgenic mice. *Anat Embryol* **206**:139–148.
23. Sibonga JD, Lotinun S, Evans GL, Pribluda VS, Green SJ, Turner RT 2003 Dose-response effects of 2-methoxyestradiol on estrogen target tissues in the ovariectomized rat. *Endocrinology* **144**:785–792.
24. Jorgensen SM, Demirkaya O, Ritman EL 1998 Three-dimensional imaging of vasculature and parenchyma in intact rodent organs with x-ray micro-CT. *Am J Physiol Heart Circ Physiol* **275**:H1103–H1114.
25. Sjogren K, Sheng M, Moverare S, Liu J-L, Wallenius K, Tornell J, Isaksson O, Jansson J-O, Mohan S, Ohlsson C 2002 Effects of liver-derived insulin-like growth factor I on bone metabolism in mice. *J Bone Miner Res* **17**:1977–1987.
26. Samuels A, Perry MJ, Goodship AE, Fraser WD, Tobias JH 2000 Is high-dose estrogen-induced osteogenesis in the mouse mediated by an estrogen receptor? *Bone* **27**:41–46.
27. McDougall KE, Perry MJ, Gibson RL, Colley SM, Korach KS, Tobias JH 2003 Estrogen receptor-alpha dependency of estrogen's stimulatory action on cancellous bone formation in male mice. *Endocrinology* **144**:1994–1999.
28. Zhou S, Turgeman G, Harris SE, Leitman DC, Komm BS, Bodine PV, Gazit D 2003 Estrogens activate bone morphogenetic protein-2 gene transcription in mouse mesenchymal stem cells. *Mol Endocrinol* **17**:56–66.
29. Korach KS 1994 Insights from the study of animals lacking functional estrogen receptor. *Science* **266**:1524–1527.
30. Lindberg MK, Alatalo SL, Halleen JM, Mohan S, Gustafsson JA, Ohlsson C 2001 Estrogen receptor specificity in the regulation of the skeleton in female mice. *J Endocrinol* **171**:229–236.
31. Denger S, Reid G, Kos M, Flouriot G, Parsch D, Brand H, Korach KS, Sonntag-Buck V, Gannon F 2001 ERalpha gene expression in human primary osteoblasts: Evidence for the expression of two receptor proteins. *Mol Endocrinol* **15**:2064–2077.
32. Kushner PJ, Agard DA, Greene GL, Scanlan TS, Shiao AK, Uht RM, Webb P 2000 Estrogen receptor pathways to AP-1. *J Steroid Biochem Mol Biol* **74**:311–317.
33. Cheung E, Acevedo ML, Cole PA, Kraus WL 2005 Altered pharmacology and distinct coactivator usage for estrogen receptor-dependent transcription through activating protein-1. *Proc Natl Acad Sci USA* **102**:559–564.

Address reprint requests to:
Sundeep Khosla, MD
5-194 Joseph
Endocrine Research Unit
Mayo Clinic College of Medicine
200 First Street SW
Rochester, MN 55905, USA
E-mail: khosla.sundeep@mayo.edu

Received in original form March 2, 2005; revised form June 13, 2005; accepted July 13, 2005.